Analyses and Design of the Highly Jointed Slopes on the Abutments of the World's Highest Railway Bridge Across the Chenab River in Jammu and Kashmir State, India

T. G. Sitharam, Srinivas Mantrala and A. K. Verma

Abstract Indian Railways have embarked on the construction of world's highest railway bridge as a part of Udhampur–Srinagar–Baramulla Rail Link Project, a major infrastructure project in India. The bridge is being constructed across the river Chenab. The bridge consists of a main span of 467 m arch bridge on the steep slopes on the banks of the river Chenab. The bridge is about 359 m above the high flood level of the Chenab River. The bridge is located in highly seismic area characterized with maximum credible earthquake with a peak horizontal acceleration of 0.36 g. Considering the iconic nature of the bridge and highly jointed rock mass, a variety of tests were conducted to assess bearing capacity of the foundations and stability of the slopes. Continuum analyses using Slide and FLAC softwares were carried out. The slopes were also checked for wedge failure and toppling failure considering the joint characteristics. The slope stabilization measures against wedge failure consist of using passive rock bolts and active prestressed rock anchors. The methodology for the design of these rock bolts and prestressed rock anchors for wedge failures is described briefly. The slopes have been successfully stabilized using the methodology discussed in this paper.

Keywords Slope stability · Railway bridge · Earthquake

T. G. Sitharam (✉)
Department of Civil Engineering, Indian Institute of Science,
Bengaluru 560012, India
e-mail: sitharam@civil.iisc.ernet.in

S. Mantrala
Afcons Infrastructure Limited, Mumbai 400053, India
e-mail: srinivas.mantrala@afcons.com

A. K. Verma
Department of Mining Engineering, Indian Institute of Technology (ISM),
Dhanbad 826004, India
e-mail: akverma@iitism.ac.in

R. Sundaram et al. (eds.), *Geotechnics for Transportation Infrastructure*,
Lecture Notes in Civil Engineering 29,
https://doi.org/10.1007/978-981-13-6713-7_2

1 Introduction

The evaluation of stability of the natural rock slopes becomes very essential for the safe design especially when the slopes are situated close to structures which are built on these slopes. The stability of a natural slope becomes more critical if the slope is situated in earthquake prone areas (Kumsar et al. 2000). Slope failures are the most common natural hazards and are mainly caused due to the additional forces due to foundations of the structures on them or rainfall induced or earthquake-induced ground shaking and associated inertial forces. Earthquakes of even a very small magnitude may trigger failure in slopes in jointed rock masses which are perfectly stable otherwise. Hence, the study of the behaviour of rock slopes in order to have a safe design of structures built on them. Though the strength of the rock plays an important role in the slope stability, geological structure of the rock often governs the stability of slopes in jointed rock masses. Geological characteristics of rock mass include location and number of joint sets, joint spacing, joint orientations, joint material and seepage pressure (Wyllie and Mah 2004). The dynamic analysis of slopes in rock masses is studied by several earlier researchers using different techniques (Kumsar et al. 2000; Hatzor et al. 2004).

Indian Railways are building the iconic Chenab bridge across the river Chenab which will be world's highest railway bridge once completed. The bridge is located in young Himalayan Mountains, which are active. The general arrangement of the bridge is indicated in Fig. 1. Out of eighteen foundations, seven foundations are coming on the slopes. The founding strata consists of highly jointed dolomite with three joint sets. The joints are closely spaced. Since the foundations are coming on the slopes, the slopes need to be designed very carefully considering the long-term stability requirements. The photograph taken at the proposed site before the commencement of the excavation of the slopes is presented in Fig. 2.

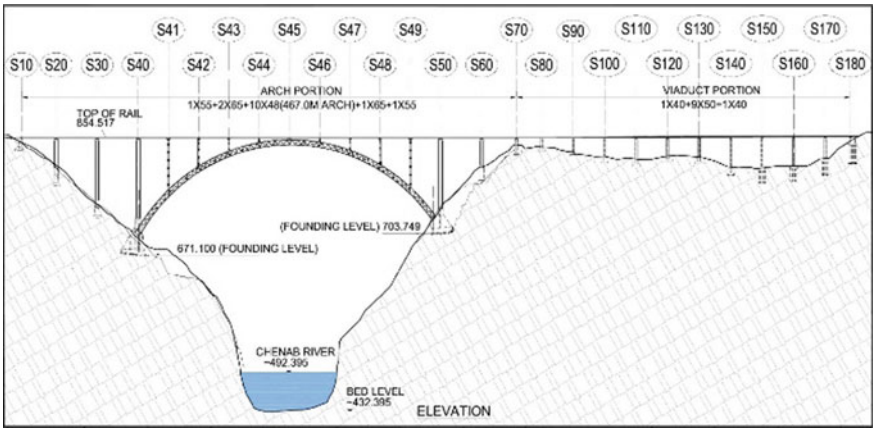

Fig. 1 The general arrangement of the bridge

Fig. 2 Left and right banks of Chenab Bridge before commencement of work

Figure 3 shows the photograph of the completed viaduct portion from S80 to S180. The portion from S130 to S180 is on transition and circular curves. For the first time in the world, the deck was launched incrementally on a combined circular and transition curves. The photograph of the deck is shown in Fig. 4. The stabilization of the slopes on both left and right banks was completed and the construction of foundations on the slopes has been completed. The photographs showing the stabilized slopes on the left and right banks are placed at Fig. 5 and Fig. 6 respectively.

Fig. 3 Completed viaduct on the right bank

Fig. 4 Incrementally launched deck on combined circular and transition curves

Fig. 5 Stabilized slopes on the left bank

Fig. 6 Stabilized slopes on the right bank

2 Rock Mass Characteristics

2.1 Joint Characteristics

The rocks present at the bridge site are heavily jointed. The subsurface at the extent of the bridge site considered for slope stability analysis essentially consists of Dolomitic limestone with different degrees of weathering and fracturing. The main discontinuities at the site are one sub-horizontal foliation joint dipping about 20°–30° in North-East (NE) direction and two sub-vertical joints. Figure 7 shows the rock mass exposed at the bridge site. The figure also depicts the intensity and spacing of the prevailing joint sets at the bridge site. Figure 8 shows the joint orientations at two drift locations.

2.2 Rock Mass Properties

After detailed analyses of geotechnical properties and in situ test results in drifts the properties for the slopes have been selected as two sets of properties, out of which one is very conservative estimate. Analyses have also been carried out treating the entire slope material as a single layer and in the other case with top disintegrated soil as a two-layer model. Tables 1 and 2 show the two sets of properties of rock mass for the continuum analyses of slope on the left bank and right bank respectively.

Fig. 7 Rock mass exposed at the bridge site

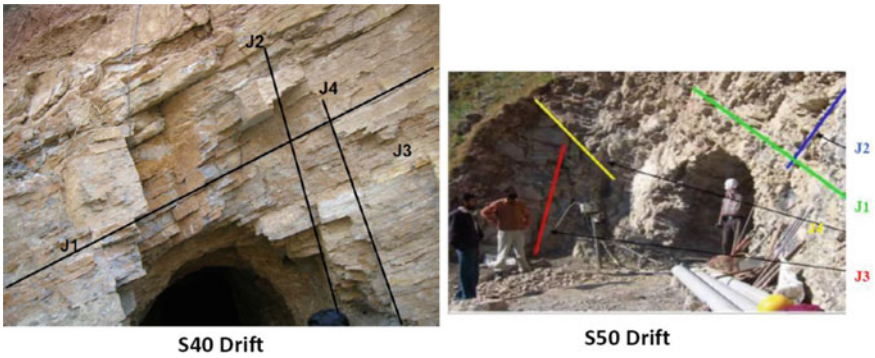

Fig. 8 Joint orientations at drift locations

Table 1 Two sets of properties of rock mass for left bank

Rock mass	Set 1	Set 2
Dry unit weight (kN/m^3)	27.095	26.752
Cohesion (c, MPa)	1.40	0.531
Friction angle (ϕ) degrees	44.42	49.10
Hoek and Brown parameter (m and s)	4.70 and 0.00127	0.793 and 0.0005
Bulk modulus (GPa)	50.55	6.31
Shear modulus (GPa)	37.92	4.73
RQD/RMR	49/48	10/37

Table 2 Two sets of properties of rock mass for right bank

Rock mass	Set 1	Set 2
Dry unit weight (kN/m^3)	27.095	27.095
Cohesion (c, MPa)	1.41	0.525
Friction angle (ϕ) degrees	42.61	49.06
Bulk modulus (GPa)	50.55	5.64
Shear modulus (GPa)	37.92	4.23
Hoek and Brown parameter (m and s)	4.706 and 0.00127	0.766 and 0.0005
RQD/RMR	49/48	10/36

3 Slope Stability Analyses

The detailed study carried out considers all possible failure modes such as global failure, wedge failure, planar failure and toppling failure. The analyses have been carried out for abutment slopes and many cross sections at both these abutment slopes. Final profile was arrived considering all the necessary alternatives, construction methodology and accessibility to the foundation locations on the slopes. The numerical programs used for the detailed slope stability analyses are as follows: Wedge failure analyses were carried out using SWEDGE (RocScience 2002); Global failure analyses using continuum approach using FLAC (Itasca 2002) and SLIDE (from Roc Science) programs; Planar failure analyses using DIPS (Roc Science 2002) and Toppling analyses using Hoek and Bray Analysis.

Analyses were carried out using two sets of rock mass properties which were decided based on large number of tests, borehole data and tests at drift locations. For the right abutment slopes, variation in rock mass properties along the slope was also considered in the continuum analyses. Lower values of moduli were considered for quartzite in the upper part of the slope. Sensitivity analyses were also done for the possible variations in shear strength parameters. There was no ground water reported during geotechnical investigations. Piezometers installed on the slope showed no head of water indicating that the water quickly drains off through the joints. However, pore pressure ratio (r_u) value of 0.3 was considered for the wedge failure analysis as decided in the design basis note. Allowable bearing pressures on foundations determined as 1 MPa (determined by several methods and after detailed deliberations) was applied at all foundations in the continuum analyses. Initially seismic analyses were done using PHA values of 0.31 g and 0.155 g for MCE and DBE cases, respectively. However, these values were increased later to 0.36 g and 0.18 g, respectively, considering the importance of the project. The earthquake response spectrum was derived for dynamic analyses using site-specific studies carried out by IIT Roorkee by multiplying a factor of 0.36 to obtain a peak horizontal acceleration of 0.36 g keeping the frequency contents and duration of the seismic event unchanged. The dynamic input is applied at the base of the slope.

Design factors of safety adopted for the slopes are as follows: FS = 1.5 with static loads; FS = 1.2 with static loads and DBE seismic loads; and FS = 1.0 with static loads and MCE seismic loads.

Using SLIDE software continuum analyses, both with circular and non-circular slip surfaces were carried out using two sets of properties as decided by the entire team and as per Design basis note. Static analyses, pseudostatic analyses with MCE loading, and pseudostatic analysis with DBE loading conditions were carried out with two sets of properties for all the slopes. Sensitivity analyses were also carried out with subset properties. Further, analyses with two-layer model considering pore water pressures were also done. Figures 9, 10, and 11 show the typical results from SLIDE analyses for some of the cases. Figures also show the factor of safety obtained for a circular slip analyses using Bishop's simplified approach for an equivalent continuum material.

Further, continuum analyses were carried out using FLAC. In this case also, static analyses, pseudostatic analyses with MCE and DBE conditions were carried out. Typical results from FLAC analyses have been presented in Figs. 12 and 13.

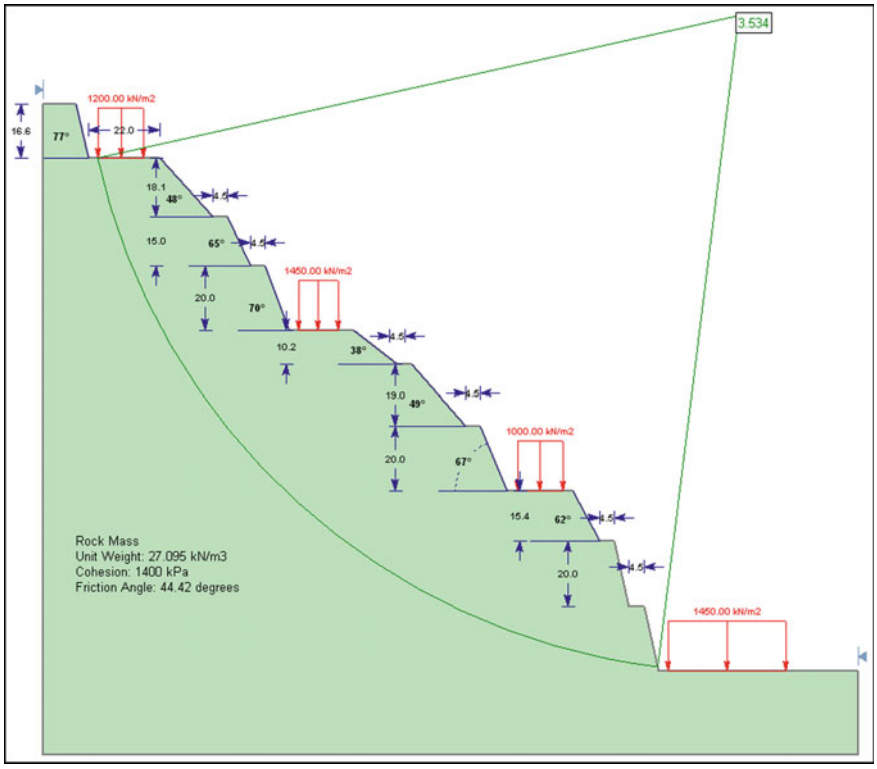

Fig. 9 Static analysis: circular global failure (FS = 3.534) using set 1 values

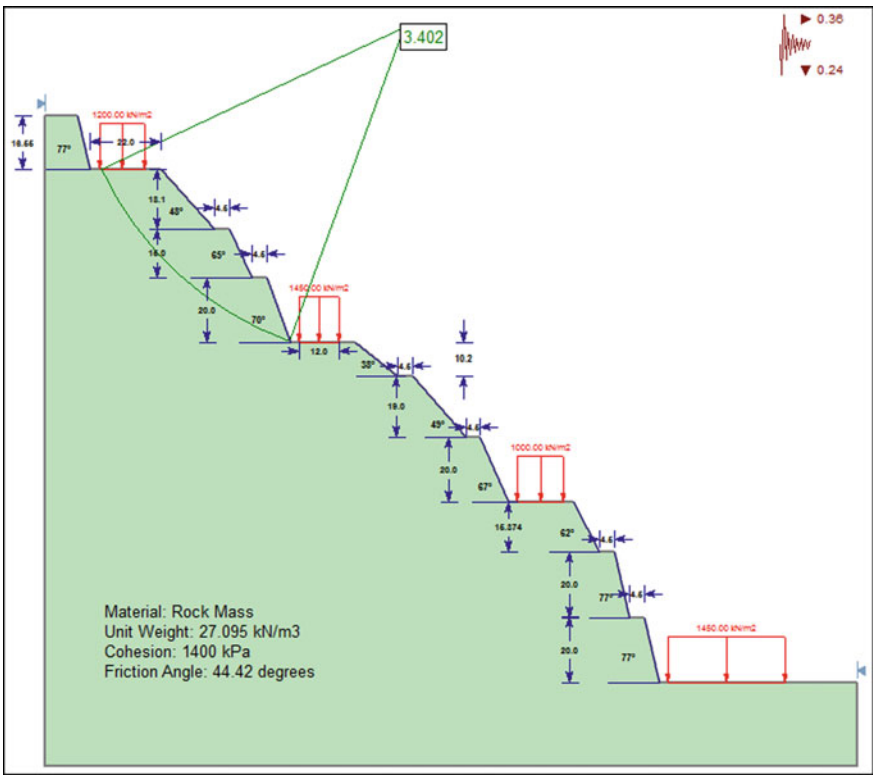

Fig. 10 Pseudostatic analysis: shallow slip failure (top), MCE condition ($\alpha h = 0.36$, $\alpha v = 0.24$) with set 1 values

From the displacement contours, the possible displacements at each founding level are tabulated and presented below in Table 3.

In addition, a dynamic analysis with MCE and DBE conditions was also carried out. Typical acceleration time history plot for MCE of the site is given in Fig. 14.

Global stability analyses with rock bolts and anchors were done to check the abutment slope up to river bed in one case and in other case 100 m below the arch foundation locations (S40 and S50).

Further for local stability considerations, a complete 3D wedge failure analysis of central and side slopes using SWEDGE was done without seismic force, and, with seismic force corresponding to MCE, with seismic force corresponding to DBE. Wedge failure analysis at different locations for different earthquake scenarios and with different friction parameters of the gouge material was analysed. Further, sensitivity analyses with three different friction angles were carried out along with

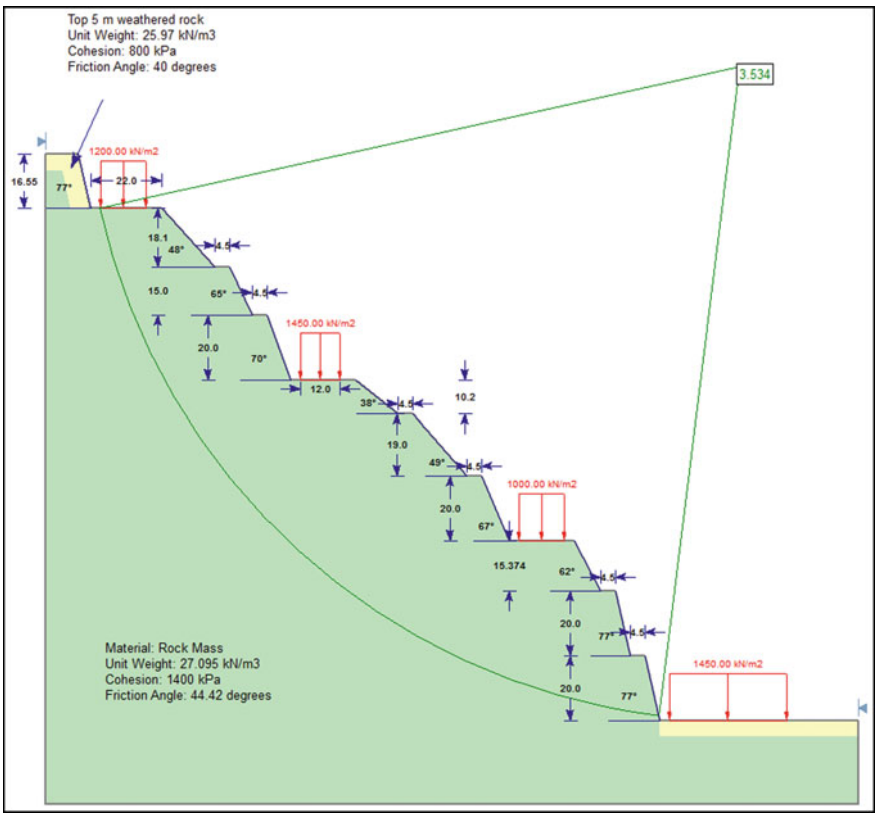

Fig. 11 Two-layered model: static analysis, circular global failure Ru coefficient = 0.3, FS = 3.534

flattened slopes to avoid any wedge failures and also analyses of slopes with rock anchors. Based on detailed analyses, appropriate strengthening measures were suggested using rock bolts and prestressed rock anchors which was executed at site.

4 Installation of Rock Bolts

4.1 Geological Logging of the Excavated Slope

After the slope is excavated, the surface is cleaned with water jet as shown in Fig. 15 and the geological log of the slope is prepared. Typical geological log is placed at Fig. 16. The data from the geological log are used for the validation of the design of slope stabilization measures.

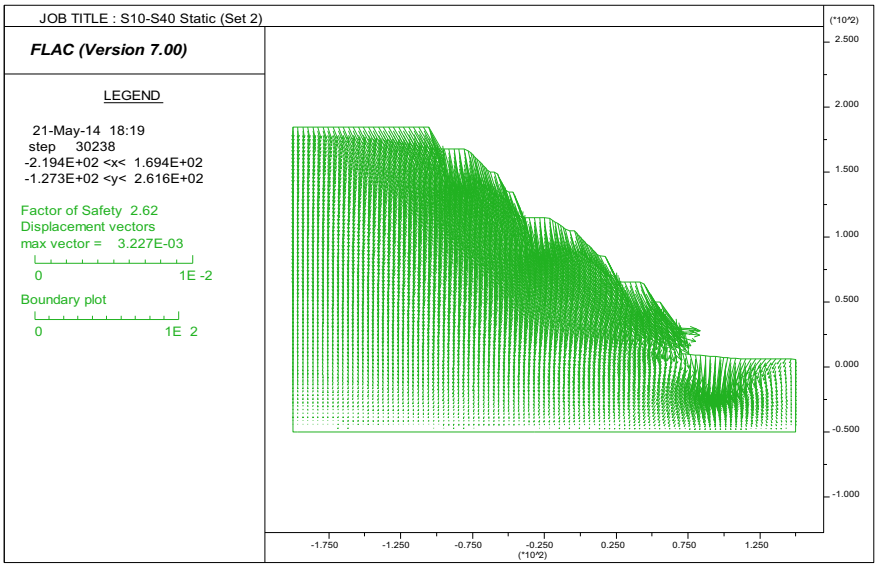

Fig. 12 Displacement vectors (FOS: 2.62, maximum displacement: 3.22 mm)

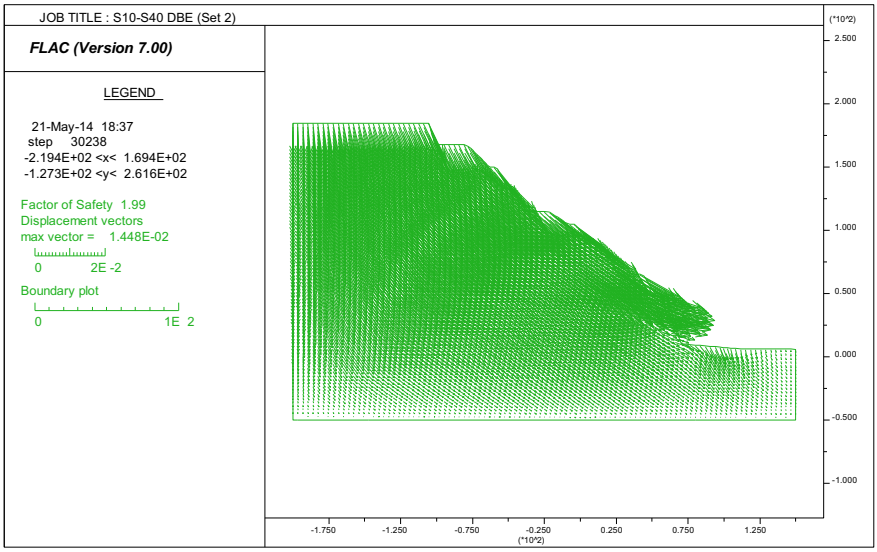

Fig. 13 Displacement vectors (FOS: 1.99, maximum displacement: 14.48 mm)—DBE CASE (seismic force coefficients: ah = 0.18; av = 0.12)

Table 3 Displacements at each founding level from FLAC analyses for foundations on Bakkal side

S.No.	Load case	Displacement type	Displacement in mm (magnitude)			
			S10	S20	S30	S40
1	Static	Lateral	0.5	0.5	1.0	−0.75
2	Static	Vertical	−3	−3	−2.5	−3.5
3	Design basis earthquake (DBE)	Lateral	2.5	7.5	10	2.5
4	Design basis earthquake (DBE)	Vertical	−9	−8	−8	−4
5	Maximum considered earthquake (MCE)	Lateral	15	20	25	5
6	Maximum considered earthquake (MCE)	Vertical	−17.5	−15	−15	−5

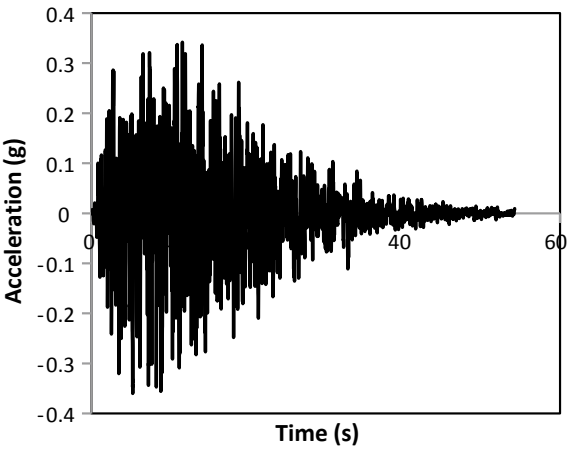

Fig. 14 Acceleration time history of the MCE for the site

4.2 Application of the First Layer of Shotcrete and Marking of Layout of Rock Bolts

After the geological logging is completed, the first layer of 50-mm-thick steel fibre reinforced shotcrete was applied as shown in Fig. 17. Later the location of rock bolt was marked on slope in accordance with the approved layout drawing.

Fig. 15 Cleaning of excavated slope with water jet

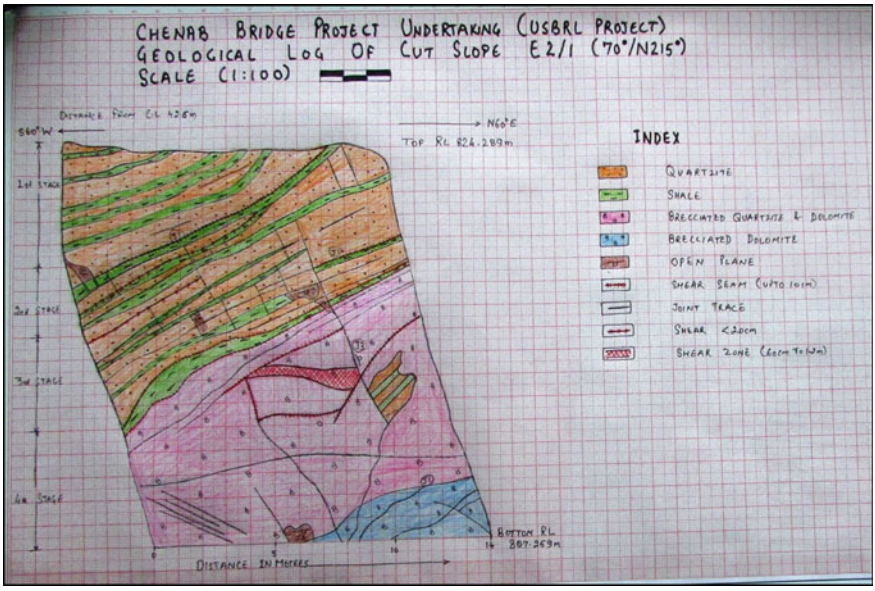

Fig. 16 Typical geological log of the excavated slope

Fig. 17 Application of 50 mm thick steel fibre-reinforced shotcrete

4.3 Drilling of Holes

Drilling of holes was done by air percussion drilling. The diameter of drilled hole was 100 mm, and the diameter of the rock bolt was 32 mm. The depth of drill hole was 300 mm more than the designed length of rock bolt. The inclination of the hole for rock bolt was perpendicular to slope. After drilling of holes, the holes were filled with neat cement grout. After the grout sets, the hole was again re-drilled.

4.4 Fabrication of Rock Bolt

Ribbed bars of 32 mm dia. of grade Fe 500 were used as rock bolts. Length of rock bolt was as per the approved drawing. The top 100 mm portion of the was threaded for fixing of M30 nut. Suitable centralizer was being fixed on the bar at spacing of 1.5 m to 2.0 m c/c to maintain clear cover to avoid bar coming in contact with ground. A mild steel plate of size 150 mm $\times$ 150 mm $\times$ 12 mm with central hole of 40 mm diameter was used as bearing plate. All rock bolts and bearing plates were coated with two coats of truncated inhibitor cement slurry to protect from corrosion.

4.5 Installation of Rock Bolts

The drilled holes were flushed by means of air jet to remove any loose materials. The rock bolt was inserted into the hole carefully along with centralizers and grout pipe. A photograph indicating the installation of rock bolts is placed at Fig. 18.

4.6 Grouting of Drill Holes

The hole was cleaned with jet of air for a period of 5 min (approx.) prior to commencement of grouting. A neat water cement grout was prepared with OPC 43/53 grade with water cement ratio of 1:0.45 as per approved grout mix design. Chemical admixture such as superplasticizer was being added to make the grout flowable; the dosages of superplasticizer will be as per grout design mix. Another chemical admixture was mixed in the grout mix to reduce shrinkage, and dosages was as per manufacturer's recommendation. The grout was mixed in high speed or colloidal mixer for about 2 min to get homogeneous and consistent mix. The flowability of grout was checked by standard flow cone of volume 1725 ml and orifice dia. 12.5 mm. The flow time of grout should be between 25 and 30 s. The minimum 28-day compressive strength of grout should be 30 MPa.

Fig. 18 Installation of rock bolts in progress

Grout mix will be pumped into hole by grout injector through grout pipe. Grouting will be done from bottom of the hole to top and grout pipe will be gradually removed as grouting progressed till fresh grout returns from the hole. After waiting for about 15–20 min, the depth of grout inside the grouted rock bolt will be checked. If there is loss of grout due to existing joints, this will be compensated by injecting additional grout inside the rock bolt hole. Once it is ensured that there is no loss of grout, the top surface of rock bolt hole will be neatly sealed with grout.

4.7 Tightening of Rock Bolt

The mild steel bearing plate of size 150 mm × 150 mm × 12 mm with central hole of dia. 40 mm was installed for the rock bolt. A 4-mm-thick plane washer was fixed on the rock bolt over base plate and tightened with M30 Nut using torque wrench to develop an axial tension equivalent to 25% design capacity of rock bolt as provided in approved drawing. Torque was applied on the rock bolts after grout attains 75% of required compressive strength which will be ascertained by conducting tests for compressive strength of grout cubes. After tightening of rock bolt, the second layer of steel fibre reinforced shotcrete is applied. The exposed portion of the rock bolt was covered by shotcrete.

4.8 Testing of Rock Bolts

The pull-out capacity of the rock bolts was ascertained by conducting pull-out tests on 1% of the working bolts. Pull-out tests were conducted up to 110% of the design capacity of the rock bolt. In the pull-out tests, there was no appreciable movement of the bolt indicating the adequacy of the design.

5 Installation of Prestressed Rock Anchors

Detailed slope stabilization analyses suggested providing prestressed bar anchors of capacity 640 kN below the foundation at S60 and prestressed cable anchors of capacity 1000 kN below the foundation S50. The finished slope below S60 foundation is shown in Fig. 19. The installation of prestressed cable anchors is in progress.

Fig. 19 Slope stabilized with prestressed bar anchors

6 Conclusions

Results from the continuum analyses using SLIDE software for both abutment slopes showed that factors of safety for all sets of properties with the are more than the required factors of safety for all the conditions considered. Similarly, the factors of safety obtained from the continuum analyses using FLAC are more than the required factors of safety for both static and pseudostatic and dynamic cases. The estimated displacements are well within the permissible limits and did not indicate any slope stabilization measures. Under dynamic loading conditions, all the displacements are less than 20 mm. Thus, differential displacements between each foundation will be far less than 20 mm which satisfies the structural design of the arch.

However, the results from the wedge failure analyses showed clearly that the factor of safety is less than required for MCE condition and warranted elaborate stabilization measures. The slopes were stabilized using both passive rock bolts and active prestressed rock anchors using both double corrosion protected prestressed bar anchors and cable anchors.

References

Hatzor YH, Arzi AA, Zaslavsky Y, Shapira A (2004) Dynamic stability analysis of jointed rock slopes using the DDA method: King Herod's Palace, Masada, Israel. Int J Rock Mech Min Sci 41(5):813–832

Itasca FLAC (2002) Fast Lagrangian Analysis of Continua, version 4.0 user's guide. Itasca Consulting Group. Inc., Thrasher Square East, p 708

Kumsar H, Aydan Ö, Ulusay R (2000) Dynamic and static stability assessment of rock slopes against wedge failures. Rock Mech Rock Eng 33(1):31–51

RocScience R (2002) Rocscience Inc. Toronto, Canada

Wyllie DC, Mah C (2004) Rock slope engineering. CRC Press